Climate Dynamics (2020) 54:117–127
https://doi.org/10.1007/s00382-019-04994-9

Amplified or exaggerated changes in perceived temperature extremes under global warming

Shuo Wang[1,2] · **Jinxin Zhu**[1]

Received: 15 June 2019 / Accepted: 19 September 2019 / Published online: 11 October 2019
© Springer-Verlag GmbH Germany, part of Springer Nature 2019

Abstract
The perceived temperature has been changing rapidly under global warming, and its related extremes have significant impacts on labor productivity and human health. Although numerous thermal indices have been developed to quantify the perceived temperature, impact assessments have not been conducted comprehensively. The lack of exploring the nonlinearity and linearity inherent in thermal indices will lead to biased conclusions. We conduct a comprehensive investigation of 161 indices to create an ensemble of selected thermal indices that represent the linear and nonlinear relationships of climatic conditions and quantify the changes in the perceived temperature and related extremes. Here we find that the increase in the mean perceived temperature can be strongly exaggerated by using nonlinear indices or linear indices that only consider the combined effect of high temperature and humidity. Wind speed incorporated into the schemes of linear indices can largely offset the increase in the perceived temperature induced by the high relative humidity. These two divergent changes can be further enhanced in future exposure to heat stress. Furthermore, our findings reveal an amplification of heatwave durations induced by the combined effects of multiple variables for all thermal indices. Such an amplification leads to a cascade of relatively short-duration heatwaves evolving into super long-lasting heatwaves which are particularly pronounced over low-latitude areas.

Keywords Perceived temperature extremes · RCPs · Climate change · Environmental health

1 Introduction

Among the global warming-induced environmental changes, one of the most detectable and definitive changes is the increase in heat extremes. It is widely believed that a combination of high temperature and high relative humidity can lead to an increased temperature perceived by the human body (Fischer and Knutti 2013; Mora et al. 2017; Willett et al. 2007; Willett and Sherwood 2012). Global climate models driven by the future scenarios of increasing CO_2 concentrations project an increase of humidity as the air temperature warming continues in the future (Frieler et al. 2011; Sherwood et al. 2010; Shiu et al. 2012). It results in the human-perceived temperature rising faster than actual air temperature (Li et al. 2018; Zhu et al. 2019). The rapid increase in perceived temperature (PT) raises serious concerns for human health [Diffenbaugh et al. 2007; (Dunne et al. 2013). Unfortunately, several challenges have hampered the global risk assessments of the fast-rising perceived temperature. First, PTs measured by thermal indices are based on the different assumptions of linear or nonlinear relationships between ambient temperature and other related variables, which have not been analyzed systematically. Second, it is unclear how these relationships can alter the characteristics of PTs and related extremes. Third, the PT changes in linear or nonlinear relationships involve a complex interplay of various atmospheric variables including air temperature (AT), relative humidity (RH), wind speed (WND), and solar radiation (SR) (de Freitas and Grigorieva 2015, 2017). For example, the equal warming under the high RH condition leads to a more significant increase in PTs through the nonlinear relationship between AT and RH than the linear relationship (Fischer and Schar 2010; Li et al.

Electronic supplementary material The online version of this article (https://doi.org/10.1007/s00382-019-04994-9) contains supplementary material, which is available to authorized users.

✉ Jinxin Zhu
jinxin.zhu@polyu.edu.hk

[1] Department of Land Surveying and Geo-Informatics, The Hong Kong Polytechnic University, Hong Kong, China

[2] The Hong Kong Polytechnic University Shenzhen Research Institute, Shenzhen, China

2018). The considerable uncertainty can lead to an exaggeration or underestimation of the exact magnitude of changes in PTs and related extremes. It is therefore crucial for conducting a comprehensive assessment of the potential risks of PTs and related extremes to inform and guide the development of long-term adaptation and mitigation strategies.

2 Methods and data

An ensemble of multiple thermal indices and general circulation models (GCMs) under different representative concentration pathway (RCP) scenarios is used to assess the impacts of climate change on PTs and related extremes, as well as to address uncertainties in indices, models and emission scenarios. A comprehensive list of 161 thermal indices (Supplementary Table S1) is assembled based on a thorough investigation of research articles. All these thermal indices calculate PTs that will result in an equivalent effect for a person as the real environment does (Staiger et al. 2012). These equivalent temperatures have the same unit as AT and, therefore, can be analyzed consistently. Suitable thermal indices were identified for this global study based on the following criteria. First, we carried out a thorough search of the available online databases for peer-reviewed publications to identify thermal indices that are experimentally tested and validated. Second, indices are excluded when they are valid only for the regional climatic context in which they are derived based on the different types of assessment scales. The assessment scale is designed to map individual index values into the categories of similar thermal sensations or stresses (Fischereit and Schlunzen 2018). Third, the indices developed for measuring the indoor thermal perception are ignored. Last, considering the extent by which PT can be modified by adaptation through physiology and behavior (Bobb et al. 2014; Gasparrini et al. 2015a; Lowe et al. 2011), body-related inputs are excluded from this study and PTs are approximated through indices that only require atmospheric inputs. Although the adaptation (such as the use of air conditioning, early warning systems, and so on) can reduce the exposure to high PTs, it will not affect the occurrence of high PTs (Mora et al. 2017; Willett and Sherwood 2012). Given the speed of current climate changes and various physiological constraints, it is unlikely that the human physiology will necessarily evolve higher heat tolerance (Hanna and Tait 2015; Mora et al. 2017; Sherwood and Huber 2010).

Among all indices evaluated, the HUM (Humidex), HEI (Heat Index), AP (Apparent Temperature), WBGT (Wet Bulb Globe Temperature), DSI (Discomfort Index), SSI (Summer Simmer Index), ESI (Environment Stress Index), NET (Net Effective Temperature), and NWB (Natural Wet Bulb Temperature) have the advantages of being well-validated and high usability for measuring PTs globally (Supplementary Text S1). Based on the linear or nonlinear relationship between AT and RH (Supplementary Fig. S1), they are categorized into two groups, namely nonlinear indices (HUM, HEI, AP, and WBGT) and linear indices (DSI, SSI, ESI, NET, and NWB). We analyze future changes in the impact-relevant PTs and extremes based on daily data from 11 GCMs (Supplementary Table S2). We focus on the highest and lowest RCP scenarios: the scenario with the most warming in which CO_2 concentrations will keep increasing through 2100 (RCP8.5) and the aggressive mitigation scenario that limits warming to below 2 °C (RCP2.6) (Taylor et al. 2012; Wang and Wang 2019). We perform a comprehensive analysis of the PT changes using nine indices, in terms of the visual comparison and the zonal averages of spatial patterns for daily PTs and related extremes in a 25-year time scale. First, we estimate the mean PT changes using multiple thermal indices and compare these changes against the mean AT increase. Then, we examine whether the linearity and nonlinearity in thermal indices can reinforce or counteract the differences between the PT changes and the AT warming. Second, we assess the sensitivities of these differences in response to uncertainties in indices, GCMs, and emission scenarios. Third, we take advantage of multiple extreme indices to assess the PT extremes and to examine whether a linear or a nonlinear relationship can lead to ununiform changes in the PT extremes across the globe. Last, we analyze the sensitivities of changes in the PT extremes in response to the different sources of uncertainty.

3 Results

Figures 1 and 2 show the simulated differences (ΔPTs) between mean PT changes (for the period 2076–2100 relative to 1980–2004) obtained by applying thermal indices and mean AT changes under two RCPs for JJA (June–July–August). ΔPTs from HUM to WBGT show consistent increases over continents (Fig. 1), indicating elevated increases in PTs when only considering the nonlinear relationship of AT and RH. This is in agreement with earlier findings (Dunne et al. 2013; Li et al. 2018; Mora et al. 2017). As for the indices considering linear relationships, there are two divergent changes in PTs. For DSI and SSI, they exacerbate ΔPTs by adding the increase of RH to the AT warming (Fig. 2). ΔPT from ESI that focuses on the combined effect of AT, RH, and SR also shows an increase over the world but with less magnitude, considering that most models simulate a decrease in SR (Wild et al. 2013, 2015). Contrarily, ΔPTs from both NET and NWB show up to 2 °C decreases over certain continents. This reveals that incorporating WND into the linear relationship can largely offset the increase in the PT induced by the high RH. While WND shows a negligible effect in the changing ΔPT obtained using AP which is a

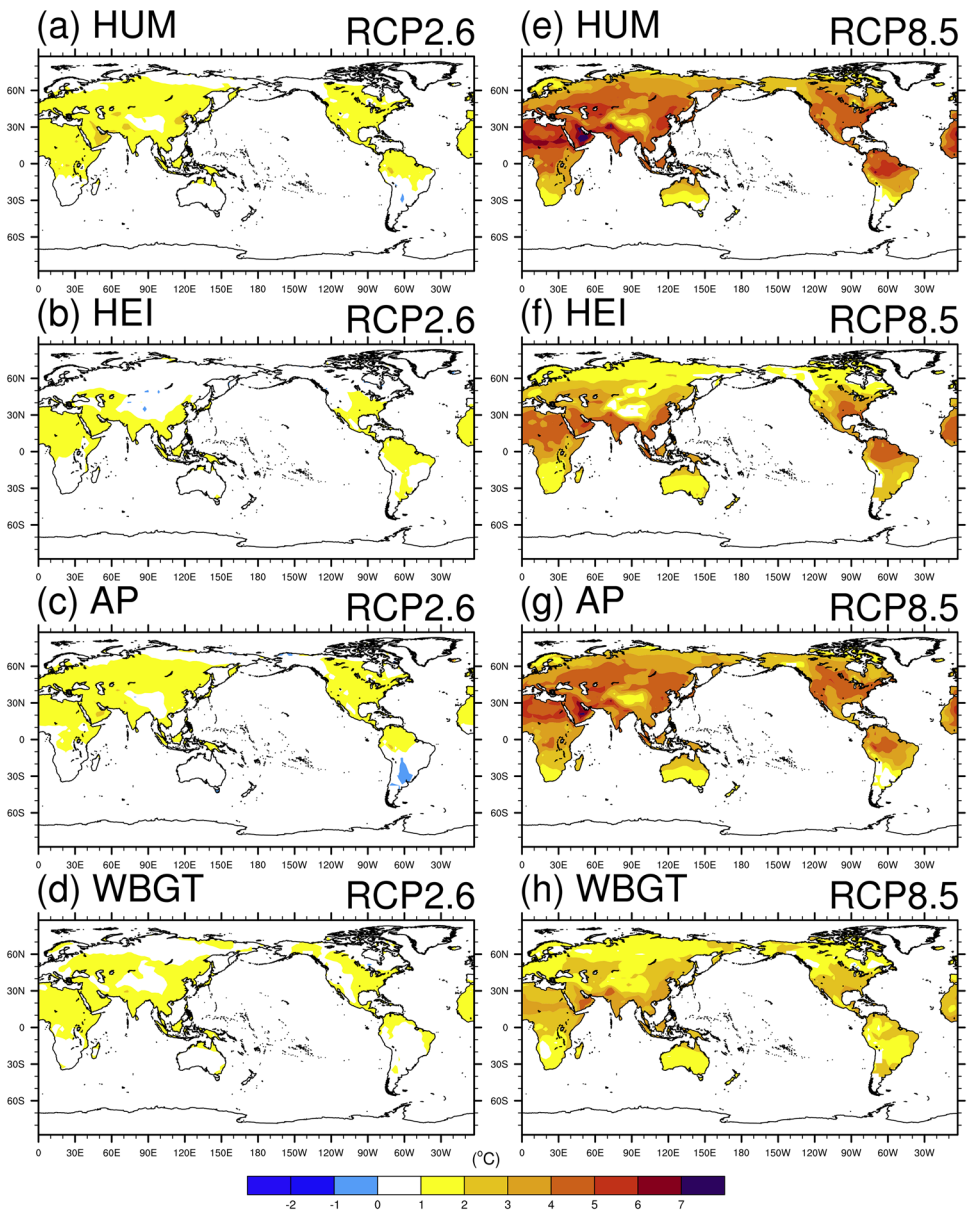

Fig. 1 ΔPT statistics of four nonlinear indices including HUM, HEI, AP, and WBGT for JJA. **a** Spatial pattern of ΔPT for 2076–2100 relative to 1980–2004 by using HUM under RCP2.6. **b–d** the same as in **a**, but using HEI (**b**), AP (**c**), WBGT (**d**) under RCP2.6; **e–h**, the same as in (**a**), but using HUM (**e**), HEI (**f**), AP (**g**), WBGT (**h**) under RCP8.5

nonlinear index considering the combined effect of AT, RH, and WND. Similar findings can be detected in the southern hemisphere for DJF (December–January–February), as shown in Supplementary Fig. S2.

Strong latitudinal gradients can be found in ΔPTs for nine indices across all land grid points between 60°S and 80°N for JJA (Fig. 3) and DJF (Supplementary Fig. S3). Results for JJA as examples, ΔPTs obtained using the nonlinear indices increase consistently from the high-latitude (> 60°N and > 60°S) to the low-latitude areas (30°S–30°N). In comparison, the results obtained using linear indices show two different gradients. For indices excluding WND, it shows that the largest increment of ΔPT over the high latitudes, the lowest increment over the middle latitudes (roughly 30°–60°), and the moderate increment over the low latitudes in the northern hemisphere. This latitudinal gradient is consistent with the spatial pattern of RH changes for the period 2076–2100 relative to 1980–2004 (Supplementary Fig. S4a). Nonlinear indices primarily amplify ΔPTs over the low-latitude areas. Linear indices, in contrast, adding the RH increases to the AT warming contribute to the largest ΔPT over the middle latitudes. For indices including WND, there are strong negative latitudinal gradients increasing from the low latitudes to the high latitudes due to the offsetting effect of WND (Supplementary Fig. S4b).

To this end, our study highlights that visually, the spatial patterns of ΔPT can be largely changed by using different thermal indices for the impact study. We compare the regional spreads of ΔPT against the spreads of mean PT changes resulting from two emissions scenarios without

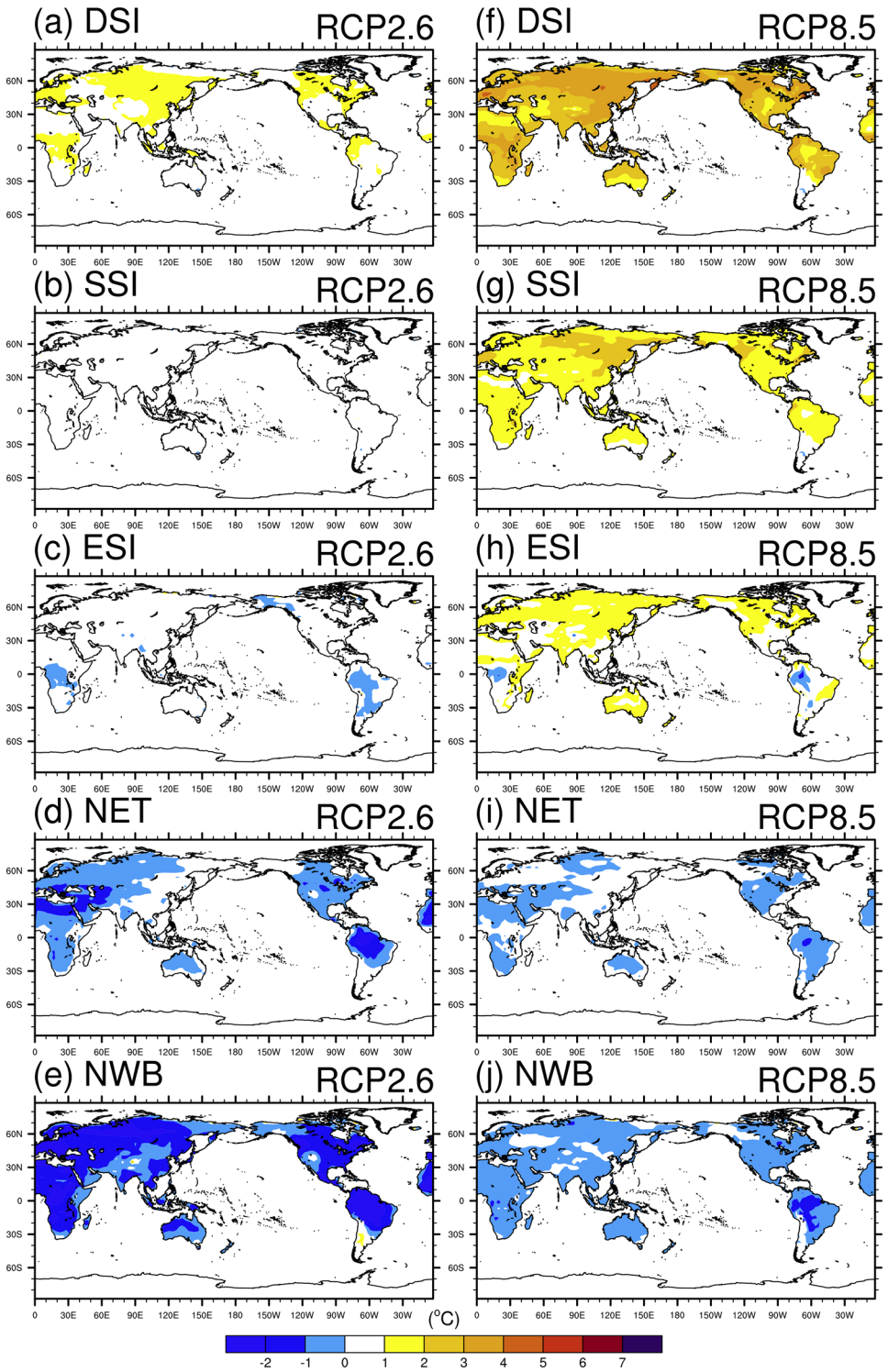

Fig. 2 ΔPT statistics of five linear indices including DSI, SSI, ESI, NET, and NWB for JJA. **a** Spatial pattern of daytime ΔPT for 2076–2100 relative to 1980–2004 by using DSI under RCP2.6. **b**–**e** the same as in **a**, but using SSI (**b**), ESI (**c**), NET (**d**), NWB (**e**) under RCP2.6; **f**–**j** the same as in **a**, but using DSI (**f**), SSI (**g**), ESI (**h**), NET (**i**), NWB (**j**) under RCP8.5

using any indices as well as against the spreads resulting from 11 GCMs for 21 regions (Supplementary Fig. S5; Table S3). It reveals that the uncertainty in indices has larger effects on the derived climate-induced PT than uncertainties in models and emission scenarios for all regions (Fig. 4). Given the high sensitivity of PT changes in response to the choice of thermal indices, one will expect biased conclusions without applying the proposed framework with a multi-index ensemble. Such biased conclusions will result in a considerable amplification or underestimation in ΔPTs.

Does the uncertainty in thermal indices prevent us from making reliable projections in the PT extremes? To explore

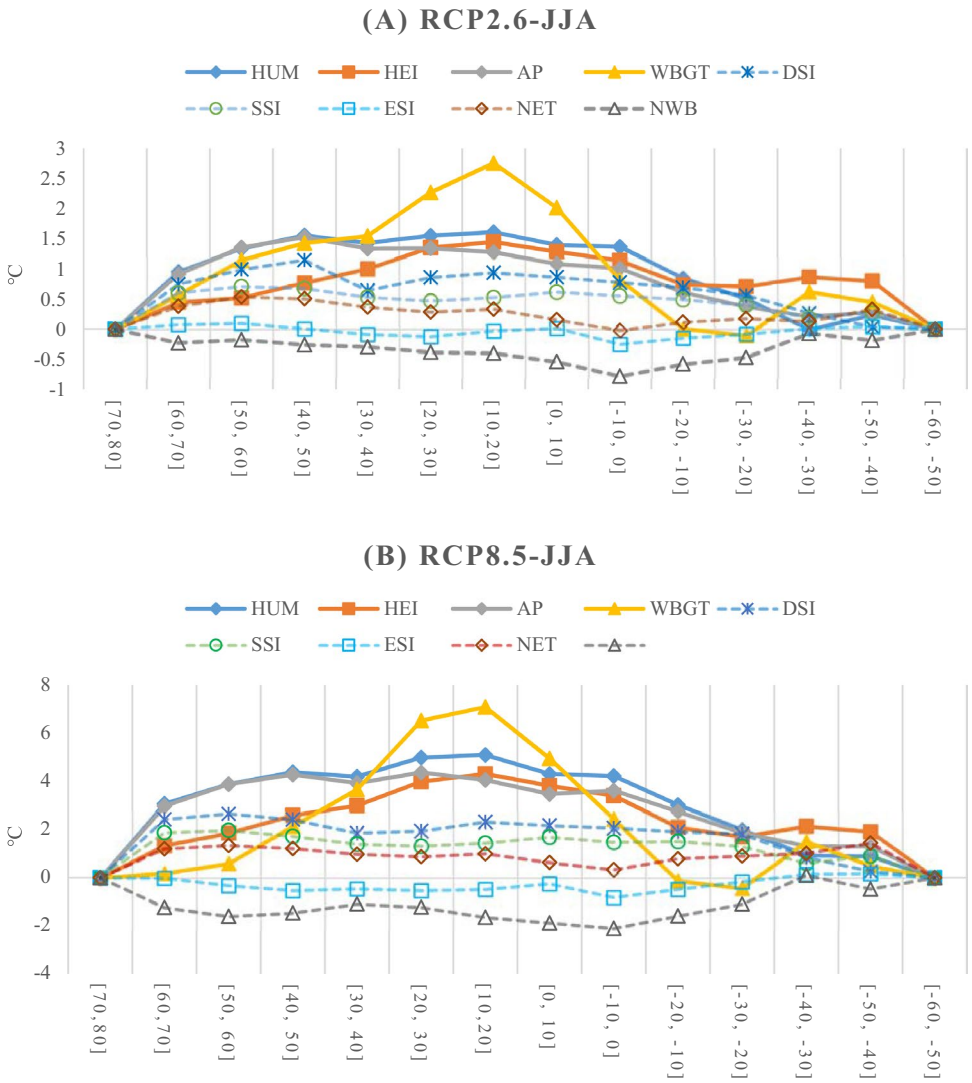

Fig. 3 Zonal average of mean ΔPT over continents under RCP2.6 (**a**) and RCP8.5 (**b**) for JJA. The blue lines are values of the multi-model ensemble mean for HUM, the orange lines for HEI, the grey lines for AP, the yellow lines for WBGT, the light blue lines for DSI, the green lines for SSI, the dark blue lines for ESI, the dark red lines for NET, the black lines for NWB

the possibility of amplifying or offsetting effects of indices on PT under extremely warming condition, we examine the contribution of different thermal indices to the change in the PT extremes. Heat stress and heatwave (Supplementary Table S4) are widely used to analyze the health-related impacts caused by temperature extremes (Fischer and Schar 2010). To investigate the effects of multiple thermal indices in changing climate extremes, here we replace ATs with PTs in the two extreme indices. Then we compare the change (for 2076–2100 relative to 1980–2004) in each extreme index calculated from PT against the change calculated from AT. The resulting difference is then analyzed to account for the significant impacts of different thermal indices on varying climate extremes.

To predict the global extent of changes in heat stress (ΔHS) induced by ΔPT, we applied the threshold of 40.6 °C (Dukesdobos 1981; Matthews et al. 2017) to the PT projections from GCMs under RCP2.6 and RCP8.5, and calculated the number of days with PTs exceeding the threshold for JJA (Figs. 5, 6) and DJF (Supplementary Fig. S6). For JJA, we find that the tropical regions (for example, tropical Africa and Southeast Asia) will be exposed to PTs exceeding the threshold by more than 20 days per year by the end of this century even under RCP2.6. Under RCP8.5, the projected number of days of surpassing the threshold is up to 60 days and increases from the middle latitudes to the equator. Nonlinear indices agree well on such a change and show a consistent pattern in ΔHS (Fig. 5). However, the greatest warming in dry regions around the equator (i.e., Sahara and the Middle East) tends to have negative changes in the days with PT exceeding the threshold. Owe to the nonlinearity in indices, ΔPT can be smaller than the magnitude of the AT warming when there is a large deficiency of moisture in the atmosphere. As for linear indices, their results exhibit inconsistent changes in ΔHS. For indices only considering the combined effect of AT and RH (Fig. 6), they generate the patterns of ΔHS close to nonlinear indices' over the humid

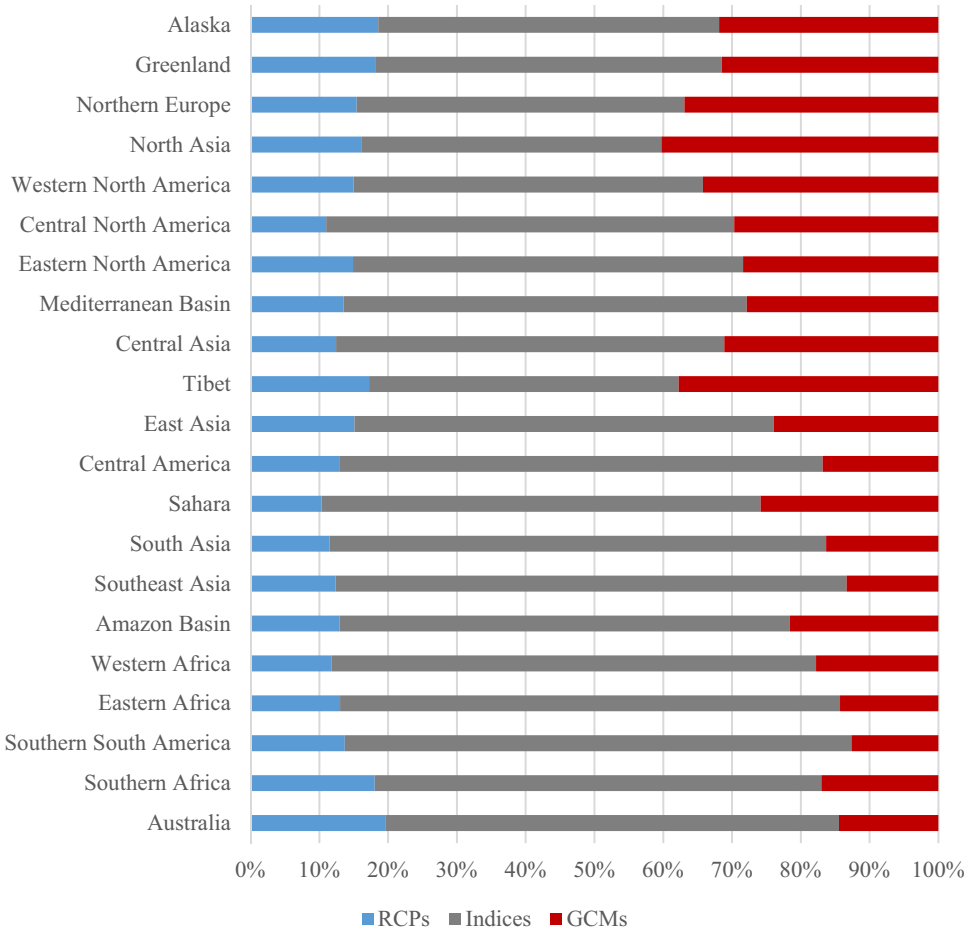

Fig. 4 Proportions of indices uncertainty (grey bars), scenario uncertainty (blue bars), and model uncertainty (red bars) contributing to the overall uncertainty in the mean PT change for 21 regions

regions. Hence, the humidity-induced heat stress amplification is strongest in the most humid and warmest regions. ΔHS derived using ESI shows positive changes over the equator but with less magnitude owing to the reduction in SR. A strong latitudinal gradient (Supplementary Fig. S7) can be found in all nine indices' results. Substantial increases in ΔHS are identified at the areas between 20°S and 20°N regardless of the linearity and nonlinearity in thermal indices. Results obtained using linear indices considering WND show decreases under RCP2.6 and RCP8.5. Substantial reductions in ΔHS (especially for NET and NWB) are found in dry regions such as Sahara, the Middle East, and Central Asia (Supplementary Fig. S8). The role of WND in reducing the heat stress over dry regions raises concerns about the liability of thermal indices. Such uncertainty from mean climate state can still result in large spreads in heat stress using thermal indices. We found that the uncertainty range resulting from indices is larger than the uncertainty ranges derived from GCMs and scenarios. Owing to the combined effects of various climatic variables, one would expect total opposite trends in PT changes with applying different thermal indices. Researchers should use linear indices with cautions, especially for indices considering WND, which can underestimate future exposure to heat stress.

Even though considerable uncertainties exist in ΔPTs as a result of various thermal indices, the spatial patterns of ΔHF (changes in the frequency of heatwave induced by ΔPT) over the land show a relatively consistent decrease across different thermal indices for JJA (Supplementary Fig. S9) and DJF (Supplementary Fig. S10). These negative changes also have a strong latitudinal gradient increasing from high latitudes to the equator (Supplementary Fig. S11). To investigate these negative changes in ΔHF, we examine the changes induced by multiple indices in total days with daily PT exceeding the 90th percentile of the reference period. The heatwave is defined to be a spell of no less than 5 consecutive days with daily temperatures exceeding the 90th percentile of the reference period, 1980–2004 (Gasparrini et al. 2015b; Johnson et al. 2018; Meehl and Tebaldi 2004; Wang et al. 2018; Zhang et al. 2019). Both linear and nonlinear indices without WND consistently amplify the percentage of days (ΔD_{90}) with PT exceeding the 90th percentile threshold compared to the days with AT exceeding the 90th percentile threshold for JJA (Supplementary Fig. S12) and DJF (Supplementary Fig. S13). There are notable negative changes in ΔD_{90} obtained

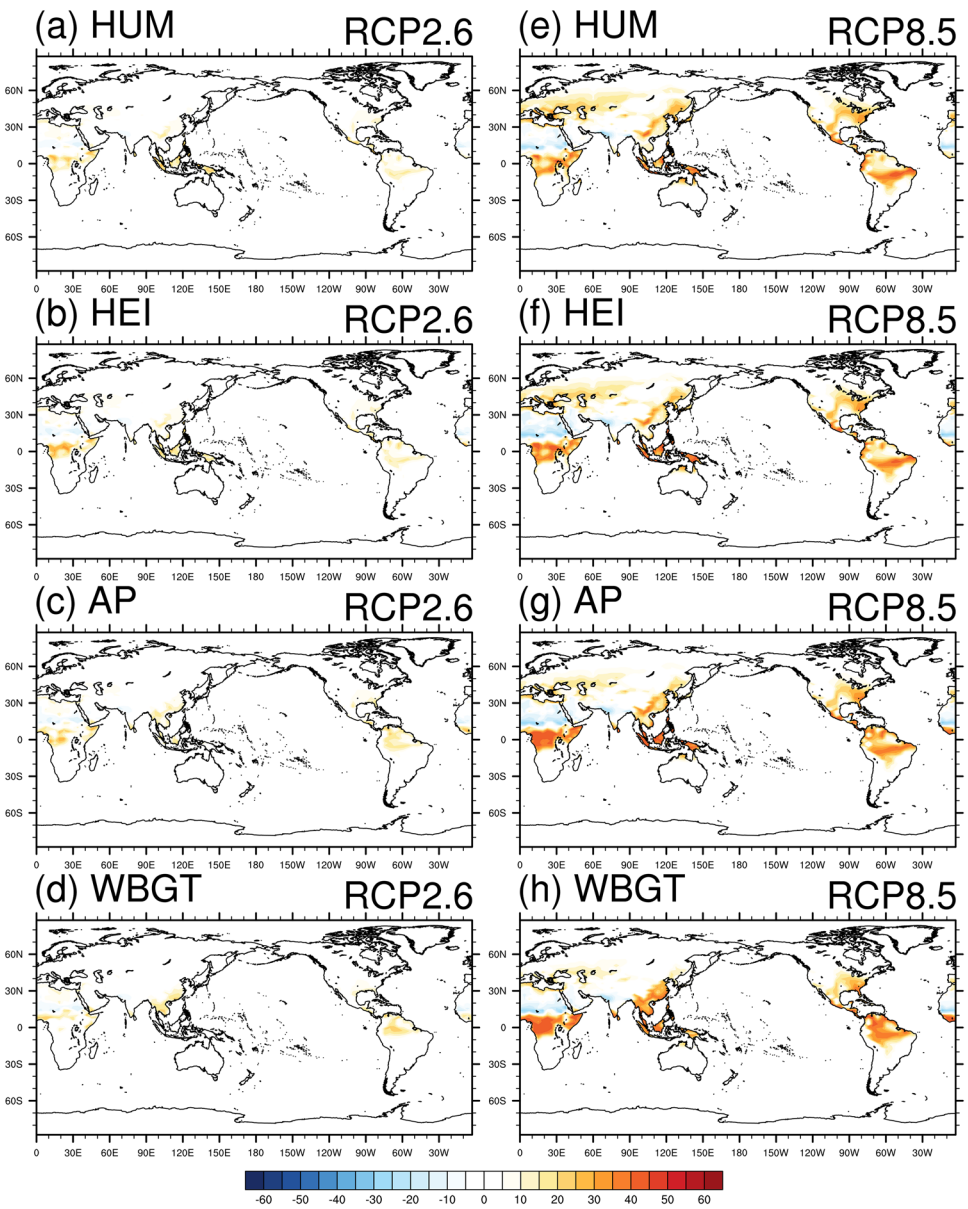

Fig. 5 Spatial pattern of ΔHS (days) for PT exceeding 40.6 °C calculated by four nonlinear indices including HUM, HEI, AP, and WBGT for JJA. **a** ΔHS induced by the ΔPT using HUM under RCP2.6 for 2076–2100 relative to 1980–2004; **b**–**d** the same as in **a**, but using HEI (**b**), AP (**c**), WBGT (**d**) under RCP2.6; **e**–**h**, the same as in **a**, but using HUM (**e**), HEI (**f**), AP (**g**), WBGT (**h**) under RCP8.5

using linear indices with WND. Therefore, the negative ΔHF for both NET and NWB is caused by the large reduction in ΔD_{90} obtained using linear indices that consider the wind chill effect. Again, considering WND in the linear relationship can lead to underestimation of future exposure to heatwaves. By 2100, the humid tropical areas (for instance, 0°–10°N) will have 20% more ΔD_{90} mainly induced by the combined effects of AT and RH. Compared to the mid- and high-latitude areas, the tropical regions have less significant seasonality, which means an increasing number of days with PT close to the 90th percentile threshold (Argueso et al. 2016). Results support the findings in previous studies that the tropical regions will expect the strongest PT amplification by using a single thermal index (Delworth et al. 1999; Fischer et al. 2012). Frequencies of heatwaves derived from the proposed framework are reduced while the total number of days with PT exceeding the 90th percentile threshold are increasing. It indicates that the duration of heatwave must be varied substantially by multiple thermal indices.

We, therefore, divide the heatwave events into six categories based on a 5-day window (namely [5, 10) consecutive days, [10, 15) consecutive days, [15 20) consecutive days, [20, 25) consecutive days, [25, 30) consecutive days, and over 30 consecutive days with PT exceeding the 90th percentile threshold) in order to examine the effect of multiple thermal indices on the changing durations. In Fig. 7, we find that various deficits in the heatwave events of less than 30 consecutive days and a large increase in the heatwave events of more than 30 consecutive days across land points between 40°N and 10°S. This indicates that a cascade of relatively

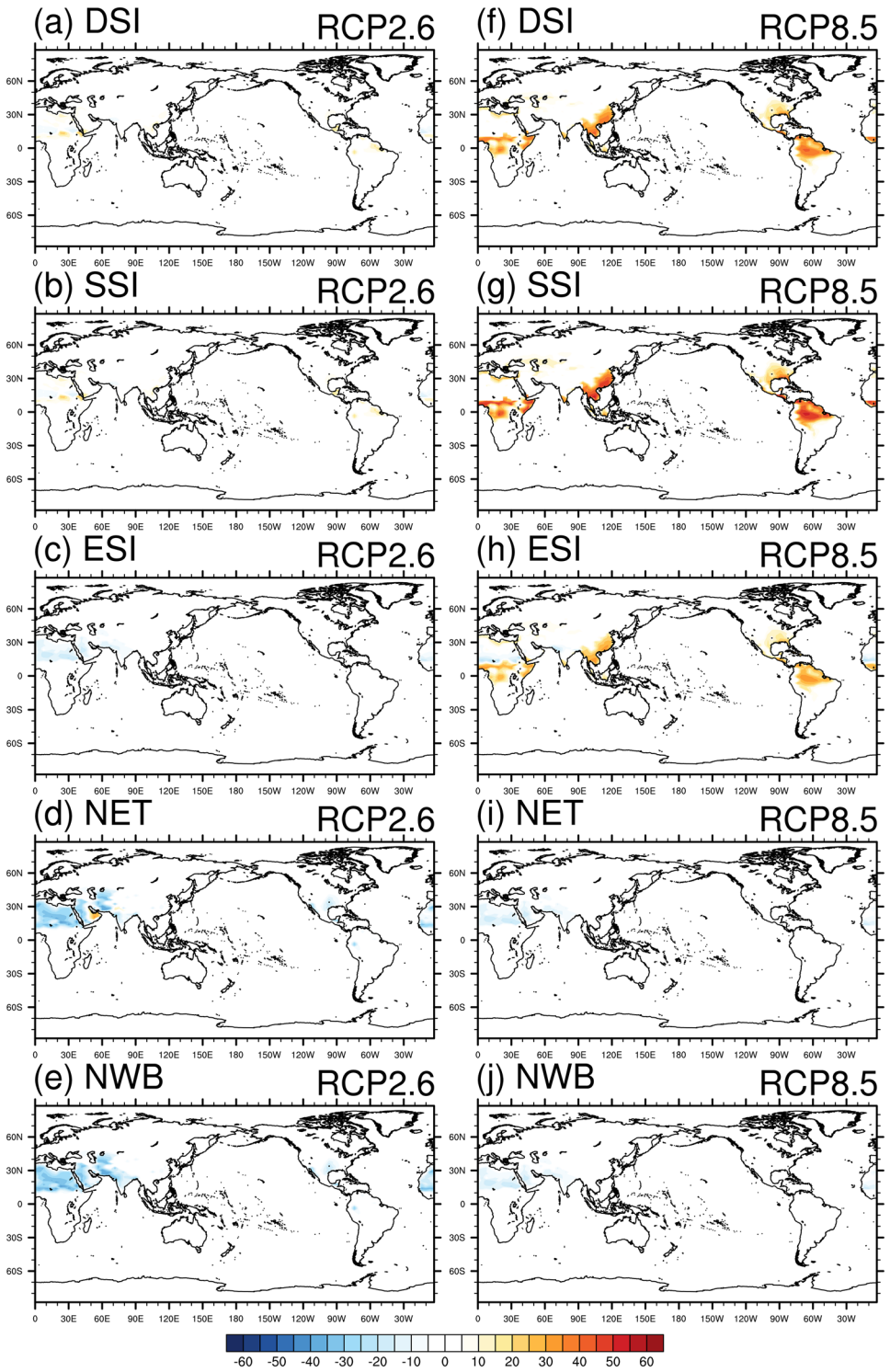

Fig. 6 Spatial pattern of ΔHS (days) for PT exceeding 40.6 °C calculated by five linear indices including DSI, SSI, ESI, NET, and NWB for JJA. **a** ΔHS induced by the ΔPT using DSI under RCP2.6 for 2076–2100 relative to 1980–2004; **b**–**e** the same as in **a**, but using SSI (**b**), ESI (**c**), NET (**d**), NWB (**e**) under RCP2.6; **f**–**j**, the same as in **a**, but using DSI (**f**), SSI (**g**), ESI (**h**), NET (**i**), NWB (**j**) under RCP8.5

short-duration heatwaves will evolve into a super long-lasting heatwave event while considering the combined effects of multiple variables. Especially, durations of heatwaves will largely increase over humid tropical areas that have the year-round hot AT with high RH and low WND. The days separating two heatwaves will require lower temperatures to exceed the 90th percentile threshold than the other areas. Therefore, the condition can be easily aggravated by the projected increases in RH and decreases in WND. As a result, there will be an increase of up to 23% in the heatwave events of more than 30 consecutive days over the tropical areas. Our findings suggest that the most densely populated regions

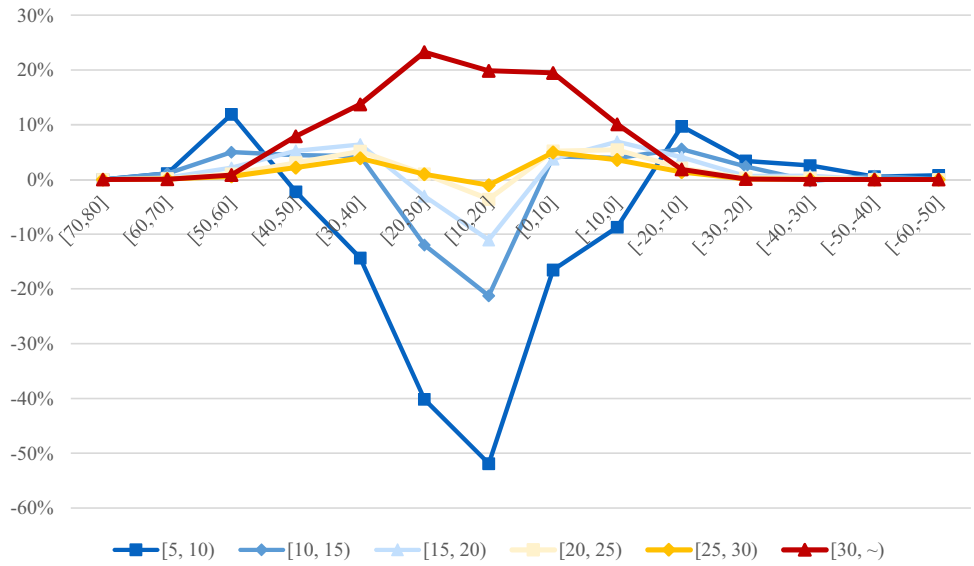

Fig. 7 Zonal average percentage changes in the durations of heatwaves over the continents for 2076–2100 relative to 1980–2004 under RCP8.5. The dark blue line represents the pattern of heatwave events of 5–10 consecutive days, the blue line for 10–15 consecutive days, the light blue line for 15–20 consecutive days, the light yellow line for 20–25 consecutive days, the yellow line for 25–30 consecutive days, and the red line for over 30 consecutive days

over the low-latitude areas, such as South Asia, Southeast Asia, and Central America (Bongaarts and O'Neill 2018; Carvalho and Wang 2019; Horton et al. 2015), can be considered as hotspots because they will experience the severest increase in the duration of perceived heatwaves.

We compare the sensitivities of changes in the PT extremes in response to uncertainties in indices, models, and emission scenarios. Across all land areas, the uncertainty range resulting from thermal indices is larger than the ranges derived from both model uncertainty and scenario uncertainty in assessing heat stress (Fig. 8). On the other hand, our results also demonstrate that all thermal indices agree well on the changes in the frequency of heatwave. Therefore, the uncertainty range from thermal indices is surprisingly low and much smaller than the ranges from model and scenario uncertainties in assessing heatwave (Supplementary Fig. S14). Linear indices considering WND tend to have negative ΔHF due to substantial reductions in their ΔD_{90}. Other thermal indices have negative ΔHF while their ΔD_{90} is increased. It should note that uncertainty in the

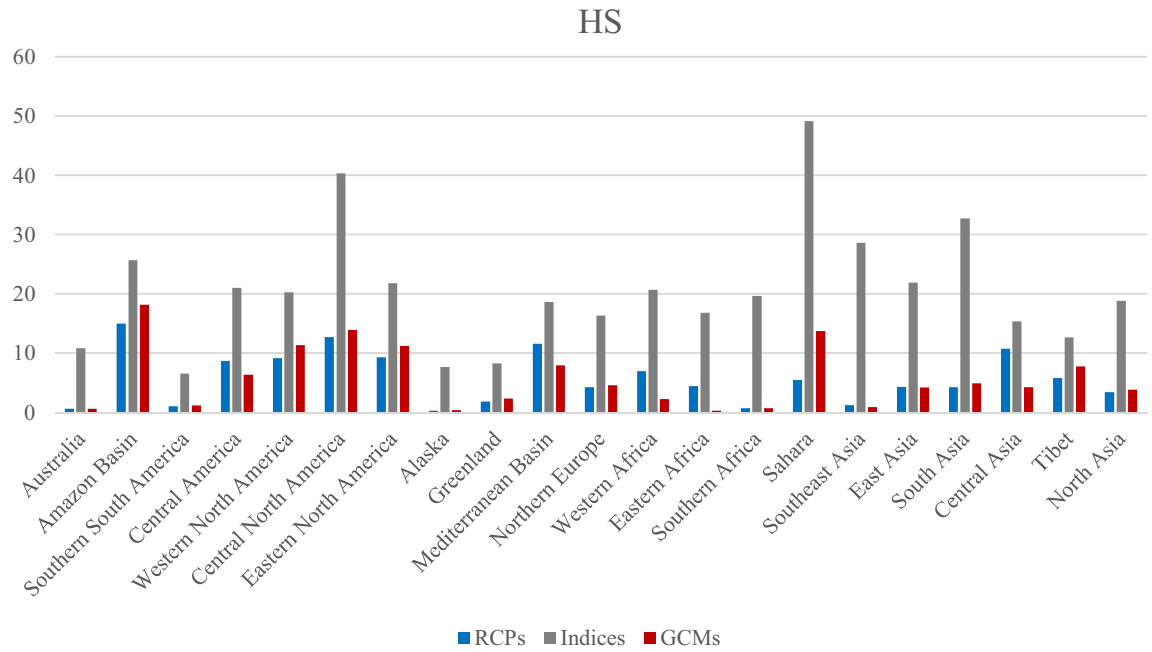

Fig. 8 Sensitivities of the extreme indices to indices uncertainty (grey bars), scenario uncertainty (blue bars), and model uncertainty (red bars): sensitivity of regional changes in percentage days with equivalent temperature exceeding 40.6 °C in response to three sources of uncertainty

frequency of heatwave can be largely reduced due to the consistently amplified durations of heatwaves other than the offsetting effect of WND.

4 Conclusions

In this study, we highlight two remarkable findings that have broad implications for assessing climate change impacts on the perceived temperature extremes. The first finding suggests that an ensemble framework of multiple thermal indices should be used to conduct a comprehensive assessment of climate change impacts on human health. The use of a single thermal index can result in biased conclusions on the mean ΔPT owing to the linearity or nonlinearity inherent in thermal indices. Compared to linear indices, nonlinear indices tend to amplify the changes in PT even while considering the offsetting effect of WND. Linear indices with or without WND can lead to opposite conclusions. Such opposite conclusions will result in a considerable amplification or underestimation of ΔPT. In addition, nonlinear and linear indices show different latitudinal gradients towards the amplification of ΔPT. Nonlinear indices largely amplify ΔPT for the areas around the equator. In contrast, linear indices that add the RH increases to the AT warming contribute to the largest ΔPT over the middle latitudes. We find that the uncertainty in thermal indices has more significant effects on the derived ΔPT than the uncertainties in model and emission scenarios for all regions.

Our second finding shows two divergent changes on PTs due to the nonlinearity and linearity inherent in thermal indices and they can be further enhanced in heat stress. For linear indices, their results are projected to increase without considering WND and to decrease with considering WND. Nonlinear indices exhibit a consistent pattern on the amplification of heat stress. Due to the nonlinearity, however, the projected large warming in dry regions over low latitudes tend to have negative changes in the days with PT exceeding the thresholds. The sensitivity of heat stress changes to the uncertainty in indices is larger than the sensitivities to model uncertainty and scenario uncertainty. It should be treated with cautions when applying thermal indices to deriving heat stress. The frequency of heatwave is projected to decrease using both linear and nonlinear indices. Our findings demonstrate that all thermal indices agree well on the changes in the frequency of heatwave due to the consistently amplified durations of heatwaves other than the offsetting effect of WND. Most thermal indices will have consistent negative changes in the frequency of perceived heatwave along with the increasing number of days with temperature exceeding the 90th percentile threshold. It results in a cascade of the frequent short-term heatwaves (less than 30 consecutive days) evolving into a super long-lasting extreme event (over 30 consecutive days) while taking into account ΔPTs derived using linear and nonlinear indices. There can be a large increase (up to 23%) in the occurrence of heatwave events of more than 30 consecutive days over tropical regions. Tropical areas will be exposed to more prolonged and severer heatwaves than ever before. Therefore, a comprehensive assessment of potential risks of PTs and related extremes is crucial to develop the long-term adaptation and mitigation strategies. The consequences of exposure to amplified HS extremes could be complicated by the problems of the aging population and increasing urbanization (Basu and Samet 2002; Kovats and Hajat 2008). Our future research work will focus on incorporating issues of aging population and urbanization to highlight areas of the planet where extreme HS conditions can be further aggravated by the population highly vulnerable to HS and the exacerbated heat-island effect.

Acknowledgements This research was supported by the National Natural Science Foundation of China (Grant no. 51809223) and the Hong Kong Polytechnic University Start-up Grant (Grant no. 1-ZE8S).

Author contributions SW and JZ conceived the study and conducted the analysis. Both authors contributed to the writing and the discussion of ideas.

Data and materials availability We acknowledge and thank the climate modeling groups (listed in Supplementary Table S2) in the World Climate Research Programme's Working Group on Coupled Modelling (which is responsible for CMIP5) for generating their model outputs and making them available. We would also like to express our sincere gratitude to the editor and anonymous reviewers for their constructive comments and suggestions.

Compliance with ethical standards

Conflict of interest We declare no competing financial interests.

References

Argueso D, Di Luca A, Perkins-Kirkpatrick SE, Evans JP (2016) Seasonal mean temperature changes control future heat waves. Geophys Res Lett 43(14):7653–7660. https://doi.org/10.1002/2016gl069408

Basu R, Samet JM (2002) Relation between elevated ambient temperature and mortality: a review of the epidemiologic evidence. Epidemiol Rev 24(2):190–202. https://doi.org/10.1093/epirev/mxf007

Bobb JF, Peng RD, Bell ML, Dominici F (2014) Heat-related mortality and adaptation to heat in the United States. Environ Health Perspect 122(8):811–816. https://doi.org/10.1289/ehp.1307392

Bongaarts J, O'Neill BC (2018) Global warming policy: is population left out in the cold? Science 361(6403):650–652. https://doi.org/10.1126/science.aat8680

Carvalho KS, Wang S (2019) Characterizing the Indian Ocean sea level changes and potential coastal flooding impacts under global warming. J Hydrol 569:373–386. https://doi.org/10.1016/j.jhydrol.2018.11.072

de Freitas CR, Grigorieva EA (2015) A comprehensive catalogue and classification of human thermal climate indices. Int J Biometeorol 59(1):109–120. https://doi.org/10.1007/s00484-014-0819-3

de Freitas CR, Grigorieva EA (2017) A comparison and appraisal of a comprehensive range of human thermal climate indices. Int J Biometeorol 61(3):487–512. https://doi.org/10.1007/s00484-016-1228-6

Delworth TL, Mahlman JD, Knutson TR (1999) Changes in heat index associated with CO_2-induced global warming. Clim Change 43(2):369–386. https://doi.org/10.1023/A:1005463917086

Diffenbaugh NS, Pal JS, Giorgi F, Gao XJ (2007) Heat stress intensification in the Mediterranean climate change hotspot. Geophys Res Lett 34:11. https://doi.org/10.1029/2007gl030000

Dukesdobos FN (1981) Hazards of heat exposure—a review. Scand J Work Environ Heat 7(2):73–83. https://doi.org/10.5271/sjweh.2560

Dunne JP, Stouffer RJ, John JG (2013) Reductions in labour capacity from heat stress under climate warming. Nat Clim Change 3(6):563–566. https://doi.org/10.1038/Nclimate1827

Fischer EM, Knutti R (2013) Robust projections of combined humidity and temperature extremes. Nat Clim Change 3(2):126–130. https://doi.org/10.1038/Nclimate1682

Fischer EM, Schar C (2010) Consistent geographical patterns of changes in high-impact European heatwaves. Nat Geosci 3(6):398–403. https://doi.org/10.1038/Ngeo866

Fischer EM, Oleson KW, Lawrence DM (2012) Contrasting urban and rural heat stress responses to climate change. Geophys Res Lett. https://doi.org/10.1029/2011gl050576

Fischereit J, Schlunzen KH (2018) Evaluation of thermal indices for their applicability in obstacle-resolving meteorology models. Int J Biometeorol 62(10):1887–1900. https://doi.org/10.1007/s00484-018-1591-6

Frieler K, Meinshausen M, von Deimling TS, Andrews T, Forster P (2011) Changes in global-mean precipitation in response to warming, greenhouse gas forcing and black carbon. Geophys Res Lett. https://doi.org/10.1029/2010gl045953

Gasparrini A et al (2015a) Temporal variation in heat-mortality associations: a multicountry study. Environ Health Perspect 123(11):1200–1207. https://doi.org/10.1289/ehp.1409070

Gasparrini A et al (2015b) Mortality risk attributable to high and low ambient temperature: a multicountry observational study. Lancet 386(9991):369–375. https://doi.org/10.1016/S0140-6736(14)62114-0

Hanna EG, Tait PW (2015) Limitations to thermoregulation and acclimatization challenge human adaptation to global warming. Int J Environ Res Public Health 12(7):8034–8074. https://doi.org/10.3390/ijerph120708034

Horton DE, Johnson NC, Singh D, Swain DL, Rajaratnam B, Diffenbaugh NS (2015) Contribution of changes in atmospheric circulation patterns to extreme temperature trends. Nature 522(7557):465–469. https://doi.org/10.1038/nature14550

Johnson NC, Xie SP, Kosaka Y, Li XC (2018) Increasing occurrence of cold and warm extremes during the recent global warming slowdown. Nat Commun. https://doi.org/10.1038/s41467-018-04040-y

Kovats RS, Hajat S (2008) Heat stress and public health: a critical review. Annu Rev Publ Health 29:41. https://doi.org/10.1146/annurev.publhealth.29.020907.090843

Li JF, Chen YQD, Gan TY, Lau NC (2018) Elevated increases in human-perceived temperature under climate warming. Nat Clim Change 8(1):43–47. https://doi.org/10.1038/s41558-017-0036-2

Lowe D, Ebi KL, Forsberg B (2011) Heatwave early warning systems and adaptation advice to reduce human health consequences of heatwaves. Int J Environ Res Public Health 8(12):4623–4648. https://doi.org/10.3390/ijerph8124623

Matthews TKR, Wilby RL, Murphy C (2017) Communicating the deadly consequences of global warming for human heat stress. Proc Natl Acad Sci USA 114(15):3861–3866. https://doi.org/10.1073/pnas.1617526114

Meehl GA, Tebaldi C (2004) More intense, more frequent, and longer lasting heat waves in the 21st century. Science 305(5686):994–997. https://doi.org/10.1126/science.1098704

Mora C et al (2017) Global risk of deadly heat. Nat Clim Change 7(7):501–506. https://doi.org/10.1038/Nclimate3322

Sherwood SC, Huber M (2010) An adaptability limit to climate change due to heat stress. Proc Natl Acad Sci USA 107(21):9552–9555. https://doi.org/10.1073/pnas.0913352107

Sherwood SC, Ingram W, Tsushima Y, Satoh M, Roberts M, Vidale PL, O'Gorman PA (2010) Relative humidity changes in a warmer climate. J Geophys Res Atmos. https://doi.org/10.1029/2009jd012585

Shiu CJ, Liu SC, Fu CB, Dai AG, Sun Y (2012) How much do precipitation extremes change in a warming climate? Geophys Res Lett. https://doi.org/10.1029/2012gl052762

Staiger H, Laschewski G, Grätz A (2012) The perceived temperature—a versatile index for the assessment of the human thermal environment. Part A: Scientific basics. Int J Biometeorol 56(1):165–176. https://doi.org/10.1007/s00484-011-0409-6

Taylor KE, Stouffer RJ, Meehl GA (2012) An overview of CMIP5 and the experiment design. Bull Am Meteorol Soc 93(4):485–498. https://doi.org/10.1175/Bams-D-11-00094.1

Wang S, Wang Y (2019) Improving probabilistic hydroclimatic projections through high-resolution convection-permitting climate modeling and Markov chain Monte Carlo simulations. Clim Dyn 53(3–4):1613–1636. https://doi.org/10.1007/s00382-019-04702-7

Wang S, Ancell BC, Huang GH, Baetz BW (2018) Improving robustness of hydrologic ensemble predictions through probabilistic pre- and post-processing in sequential data assimilation. Water Resour Res 54(3):2129–2151. https://doi.org/10.1002/2018wr022546

Wild M, Folini D, Schar C, Loeb N, Dutton EG, Konig-Langlo G (2013) The global energy balance from a surface perspective. Clim Dyn 40(11–12):3107–3134. https://doi.org/10.1007/s00382-012-1569-8

Wild M, Folini D, Henschel F, Fischer N, Muller B (2015) Projections of long-term changes in solar radiation based on CMIP5 climate models and their influence on energy yields of photovoltaic systems. Sol Energy 116:12–24. https://doi.org/10.1016/j.solener.2015.03.039

Willett KM, Sherwood S (2012) Exceedance of heat index thresholds for 15 regions under a warming climate using the wet-bulb globe temperature. Int J Climatol 32(2):161–177. https://doi.org/10.1002/joc.2257

Willett KM, Gillett NP, Jones PD, Thorne PW (2007) Attribution of observed surface humidity changes to human influence. Nature 449(7163):710-U716. https://doi.org/10.1038/nature06207

Zhang B, Wang S, Wang Y (2019) Copula-based convection-permitting projections of future changes in multivariate drought characteristics 124(14):7460–7483. https://doi.org/10.1029/2019jd030686

Zhu J, Wang S, Huang G (2019) Assessing climate change impacts on human-perceived temperature extremes and underlying uncertainties. J Geophys Res Atmos 124(7):3800–3821. https://doi.org/10.1029/2018jd029444

Publisher's Note Springer Nature remains neutral with regard to jurisdictional claims in published maps and institutional affiliations.